Digestion

Research Article

Digestion
DOI: 10.1159/000512575

Received: December 23, 2019
Accepted: October 26, 2020
Published online: January 4, 2021

S100P Expression via DNA Hypomethylation Promotes Cell Growth in the Sessile Serrated Adenoma/Polyp-Cancer Sequence

Sayo Takahashi[a] Koichi Okamoto[a] Toshihito Tanahashi[a] Shota Fujimoto[a] Tadahiko Nakagawa[a] Masahiro Bando[a] Beibei Ma[a] Tomoyuki Kawaguchi[a] Yasuteru Fujino[a] Yasuhiro Mitsui[a] Shinji Kitamura[a] Hiroshi Miyamoto[a] Yasushi Sato[a] Naoki Muguruma[a] Yoshimi Bando[b] Toshiro Sato[c] Takahiro Fujimori[d] Tetsuji Takayama[a]

[a]Department of Gastroenterology and Oncology, Institute of Biomedical Sciences, Tokushima University Graduate School, Tokushima, Japan; [b]Division of Pathology, Tokushima University Hospital, Tokushima, Japan; [c]Department of Gastroenterology, Keio University School of Medicine, Tokyo, Japan; [d]Diagnostic Pathology Center, Shinko Hospital, Kobe, Japan

Keywords
Sessile serrated adenoma/polyp · DNA hypomethylation · S100P · 3-dimensional organoid · Genome-wide DNA methylation array

Abstract
Background/Aims: Sessile serrated adenomas/polyps (SSA/Ps) are a putative precursor lesion of colon cancer. Although the relevance of DNA hypermethylation in the SSA/P-cancer sequence is well documented, the role of DNA hypomethylation is unknown. We investigated the biological relevance of DNA hypomethylation in the SSA/P-cancer sequence by using 3-dimensional organoids of SSA/P. ***Methods:*** We first analyzed hypomethylated genes using datasets from our previous DNA methylation array analysis on 7 SSA/P and 2 cancer in SSA/P specimens. Expression levels of hypomethylated genes in SSA/P specimens were determined by RT-PCR and immunohistochemistry. We established 3-dimensional SSA/P organoids and performed knockdown experiments using a lentiviral shRNA vector. DNA hypomethylation at CpG sites of the gene was quantitated by MassARRAY analysis. ***Results:*** The mean number of hypomethylated genes in SSA/P and cancer in SSA/P was 41.6 ± 27.5 and 214 ± 19.8, respectively, showing a stepwise increment in hypomethylation during the SSA/P-cancer sequence. S100P, S100α2, PKP3, and MUC2 were most commonly hypomethylated in SSA/P specimens. The mRNA and protein expression levels of S100P, S100α2, and MUC2 were significantly elevated in SSA/P compared with normal colon tissues, as revealed by RT-PCR and immunohistochemistry, respectively. Among these, mRNA and protein levels were highest for S100P. Knockdown of the S100P gene using a lentiviral shRNA vector in 3-dimensional SSA/P organoids inhibited cell growth by >50% ($p < 0.01$). The mean diameter of SSA/P organoids with S100P gene knockdown was significantly smaller compared with control organoids. MassARRAY analysis of DNA hypomethylation in the S100P gene revealed significant hypomethylation at specific CpG sites in intron 1, exon 1, and the 5′-flanking promoter region. ***Conclusion:*** These results suggest that DNA hypomethylation, including S100P hypomethylation, is supposedly associated with the SSA/P-cancer sequence. S100P overexpression via DNA hypomethylation plays an important role in promoting cell growth in the SSA/P-cancer sequence.

karger@karger.com
www.karger.com/dig

Tetsuji Takayama
Department of Gastroenterology and Oncology
Institute of Biomedical Sciences, Tokushima University Graduate School
3-18-15 Kuramoto-cho, Tokushima 770-8503 (Japan)
takayama@tokushima-u.ac.jp

Introduction

Colorectal cancer (CRC) is one of the leading causes of cancer-related death worldwide [1]. Although the adenoma-carcinoma sequence is thought to be a major pathway in colorectal carcinogenesis, the serrated-neoplasia pathway, in which serrated polyps give rise to cancers, has been the subject of recent interest as an alternative pathway of CRC development [2–5]. The serrated-neoplasia pathway reportedly accounts for approximately 15–30% of CRCs [3, 4, 6]. Serrated polyps (lesions) are mainly classified into 3 subtypes [7, 8]: hyperplastic polyp, sessile serrated adenoma/polyp (SSA/P), and traditional serrated adenoma (TSA). Of these, SSA/P has been recognized as a precursor lesion of CRC, characterized by BRAF mutation, CpG island methylator phenotype, and microsatellite instability [9–12]. Several investigators have reported that hypermethylation of various genes including p16, MINT, and MLH1 in the CpG island was associated with development of SSA/P [13–16]. We performed a genome-wide methylation array analysis and found that hypermethylation and silenced expression of several genes including PQLC1, HDHD3, RASL10B, FLI1, GJA3, and SLC26A2 were closely associated with development of SSA/P [17]. Moreover, recently Liu and colleagues [18] reported that novel 20 genes had been hypermethylated during the process of dysplasia formation in SSA/P. In contrast with DNA hypermethylation, however, fewer studies on DNA hypomethylation in CRC and other cancers have been reported. In CRC, hypomethylation of long interspersed nucleotide element-1 has been observed to a varying degree [19, 20]. Moreover, Cui and colleagues [21] reported that loss of imprinting of insulin-like growth factor 2 and H19 is initiated by DNA hypomethylation in CRCs, implicating a role of DNA hypomethylation in colorectal carcinogenesis. There has been only 1 published study involving DNA hypomethylation in SSA/P tissues. Renaud and colleagues [22] reported hypomethylation of MUC5AC in SSA/P tissues as well as in microvesicular hyperplastic polyps. However, no other studies on DNA hypomethylation have been reported in SSA/P tissues, and therefore, the role of DNA hypomethylation in the serrated-neoplasia pathway has remained unknown.

In the present study, we investigated hypomethylated genes with genome-wide DNA hypomethylation array analyses in SSA/P and cancer in SSA/P specimens to clarify the biological relevance of DNA hypomethylation in the SSA/P-cancer sequence of CRC. Since we ultimately found that S100P is commonly hypomethylated and overexpressed in SSA/P tissues, we then investigated the role of S100P in the SSA/P-cancer sequence by establishing 3-dimensional organoids from SSA/P. Moreover, we examined the detailed mechanism by which transcription of the S100P gene is increased.

Patients and Methods

Patients and Samples

We previously performed a genome-wide DNA methylation array analysis on 7 SSA/P and 2 cancer in SSA/P specimens using the microarray-based integrated analysis of methylation by isoschizomers (MIAMI) method and analyzed the hypermethylated genes region [17]. In the present study, we analyzed the hypomethylated genes region using those datasets. We then enrolled 11 additional patients with SSA/P and obtained 11 SSA/P tissue samples from them by biopsy or endoscopic mucosal resection for RT-PCR, immunohistochemistry, MassARRAY analysis, and organoid culture. All patients had been known or suspected to have SSA/P lesions in the colon and were referred to our hospital for endoscopic removal. The histological diagnosis of SSA/P was made independently by 2 pathologists (T.F. and Y.B.) according to the WHO criteria [7, 8]. Only lesions diagnosed as SSA/P concordantly by the pathologists were used. The baseline characteristics of all patients with SSA/P and cancer in SSA/P are described in online suppl. Table 1; see www.karger.com/doi/10.1159/000512575 for all online suppl. material.

Methylation Array Analysis

We performed methylation array analysis using MIAMI method as described in the previous report [17] and examined hypomethylation of 15,883 genes in 7 SSA/P tissues and 2 cancer in SSA/P tissues. Out of the all hypomethylated genes, we selected several genes that showed high positivity rate among the 7 SSA/P samples.

Real-Time Quantitative PCR

Total RNA was extracted using RNeasy Mini kit (Qiagen, Hilden, Germany) and reverse transcribed into complementary DNA. Probes and primers were from TaqMan gene expression assay reagents (Applied Biosystems). The following TaqMan gene expression assays were used: S100P (Hs00195584_m1; Applied Biosystems), MUC2 (Hs00159374_m1), S100α2 (Hs00195582_m1), PKP3 (Hs00170887_m1), and 18s (Hs99999901_s1) as internal controls. qRT-PCR was performed on a 7500

Real Time PCR System (Applied Biosystems). PCR amplification conditions were 1 cycle at 50°C for 2 min and 95°C for 10 min, followed by 40 cycles of 95°C for 15 s and 60°C for 1 min. The relative gene expression was determined using comparative Ct method with 18s gene as an internal control.

Immunohistochemistry

Immunohistochemical staining was performed using the streptavidin-biotin-peroxidase method with labelled streptavidin-biotin (Dako, Kyoto, Japan), as we described previously [17]. Rabbit anti-human S100P polyclonal antibody (diluted 1:1,000; Novus Biologicals, Littleton, CO, USA), rabbit anti-human MUC2 polyclonal antibody (Abcam, Cambridge, UK), rabbit anti-human S100α2 polyclonal antibody (Abcam), and rabbit anti-human PKP3 polyclonal antibody (Abcam) were used as primary antibodies.

Isolation of Intestinal Crypts and 3D Organoid Culture

We obtained biopsy specimens of SSA/P as well as normal colonic mucosa for organoid culture under colonoscopy and then removed the lesion using endoscopic mucosal resection, which was used for pathological diagnosis of SSA/P. Isolation and dissociation of stem cells from SSA/P and normal colonic tissues were performed as we described previously [23]. In brief, isolated SSA/P and normal colon cells were embedded in Matrigel (Corning Inc., New York, NY, USA) on ice and seeded in 48-well plates. The Matrigel was polymerized for 10 min at 37°C, and 250 μL/well basal culture medium including various growth factors was overlaid. We confirmed that the organoid cells were positive for BRAF codon 600 mutation (V600E), identical to the BRAF mutation in the SSA/P tissue from which 2 strains of the organoid were established (SSA/P organoids 1 and 2; online suppl. Fig. 1).

Cell Culture

Human colon cancer cell lines with BRAF mutation, HT29 and WiDr, were purchased from American Tissue Culture Collection. These cell lines were chosen for this study because they are positive for BRAF mutation and CpG island methylator phenotype, similar to findings in cancers derived from SSA/P. They were grown in RPMI 1640 medium supplemented with 10% FBS at 37°C with 5% CO_2.

Transduction of Lentiviral shRNA

We transfected a lentiviral shRNA targeting S100P to knockdown the S100P gene in SSA/P organoid, as described previously [24]. Briefly, the pLKO.1-puro vector targeting S100P (clone #1, TRCN54028; clone#2, TRCN54029) or pLKO.1-puro non-target shRNA (Sigma-Aldrich) as a control vector was mixed with lentivector packaging plasmid DNA mix and co-transfected into HEK293 cells. The viral supernatant was collected and stored at −80°C. The SSA/P organoid cells were infected with lentiviral S100P shRNA vector, and puromycin selection was performed. These assays were performed in sextuplicate.

Cell Viability Assay

Organoid cells infected with lentiviral S100P shRNA vector or control shRNA vector were seeded in 48-well plates and incubated for 7 days at 37°C. Organoid cell viability was determined by CellTiter-Glo® assay (Promega, Madison, WI, USA), as previously described [25].

Regarding the cell lines, HT29 and WiDr cells were transfected with small interfering RNA (siRNA) targeting S100P (Cell Signaling Technology Inc., Danvers, MA, USA) or random siRNA (Cell Signaling Technology) using transfection reagent, as we described previously [26]. After 24 h, the medium was replaced with normal medium and incubated for 72 h, and cell viability was determined using a cell proliferation assay. These assays were performed in sextuplicate.

Quantitative Analysis of DNA Hypomethylation by MassARRAY

Quantitative DNA methylation analysis for the S100P gene was performed by MassARRAY EpiTYPER assay, as described previously [27]. Cellular DNA was extracted from SSA/P and normal colonic mucosa tissues and treated with sodium bisulfite using an EZ DNA Methylation Kit (Zymo Research, Orange, CA, USA). In the MIAMI methylation array analysis, only probe D located in intron 1 showed significant hypomethylation, while the other probes including probe C in the 5′-flanking promoter region did not (online suppl. Table 2). Moreover, Sato and colleagues [28] suggested that the transcription regulatory region of S100P exists in the gene from exon 1 to the 5′-flanking region. Therefore, we designed 3 pairs of primers that cover the region from intron 1 (probe D), exon 1, and the 5′-flanking promoter region including 18 CpG sites (online suppl. Table 3). The reverse primer has a T7 promoter tag for in vitro transcription (5′-cagtaatacgactcactatagggagaaggct-3′), and the forward primer was tagged with a 10-mer to balance the Tm (5′-aggaagagag-3′). Bisulfite-treated DNA was amplified using the primers and treated with shrimp alka-

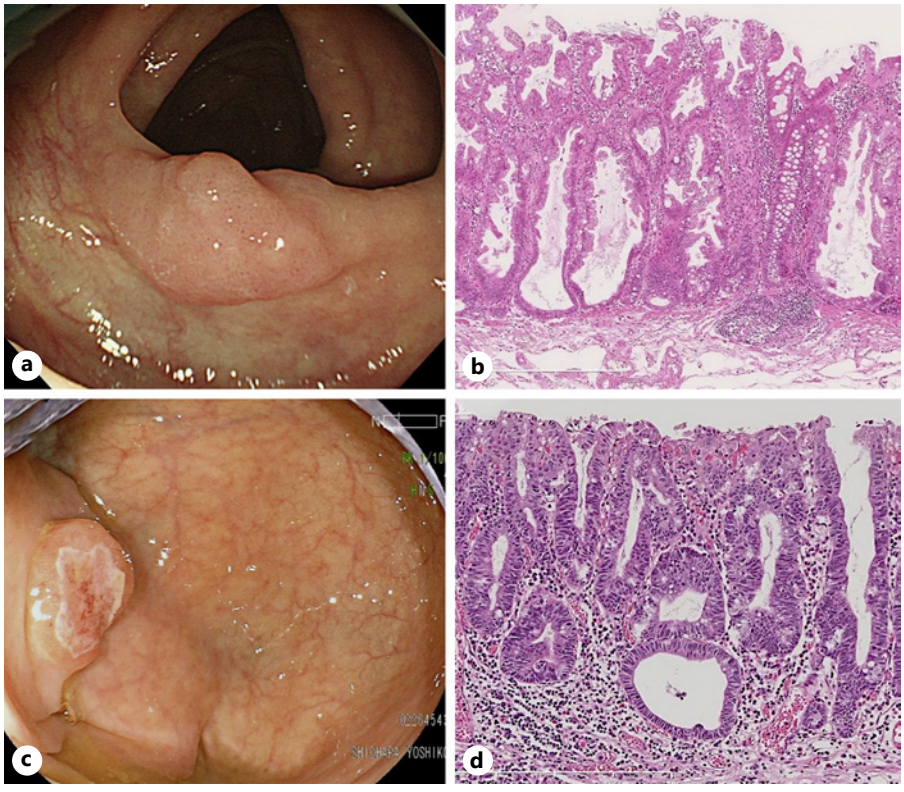

Color version available online

Fig. 1. Endoscopic and histologic features in sessile serrated adenoma/polyp (SSA/P) and cancer in SSA/P. **a** Representative endoscopic view of SSA/P with 15 mm diameter from case S1. The size was measured using biopsy forceps. **b** Histological examination showed serration with distorted and dilated crypts (H&E staining; magnification, ×100). **c** Representative endoscopic view of cancer in SSA/P with a depressed surface in the cecum from case C1. **d** Histological examination showed increased glandular density with crowded glands that had a back-to-back growth pattern and cells with rounded nuclei, coarse chromatin, and loss of polarity (H&E staining; magnification, ×100).

line phosphatase (SAP) and in vitro transcription was performed. After RNAase A digestion, small RNA fragments with CpG sites were obtained and analyzed using a MassARRAY system matrix-assisted laser desorption/ionization-time-of-flight mass spectrometer (Agena Bioscience, San Diego, CA, USA). The spectra's methylation ratios were calculated using EpiTYPER software v1.3. Universally methylated DNA from HCT116 cells (EpiScope® Methylated HCT116 gDNA; Takara Bio Inc., Mountain View, CA, USA) and unmethylated DNA from HCT116 cells (EpiScope® Unmethylated HCT116 gDNA) were used as methylation-positive and methylation-negative controls, respectively. The hypomethylation rate in each CpG site was calculated as follows: (methylation rate in normal colonic tissue – methylation rate in SSA/P tissue)/methylation rate in normal colonic tissue.

Statistics

The total number of hypomethylated genes for SSA/P and cancer in SSA/P was compared using Mann-Whitney U test. Levels of mRNA in SSA/P and normal colonic tissues were also compared using Mann-Whitney U test. Cell viability in SSA/P organoid transfected with shRNA against S100P and with control shRNA was compared using Student's *t* test, as was relative hypomethylation between normal colon and SSA/P samples.

Results

Endoscopic and Histologic Appearance of SSA/P and Cancer in SSA/P

Figure 1a shows the typical endoscopic appearance of SSA/P, with flat shape and similar color to the surrounding mucosa in the ascending colon. Histological examination of this lesion revealed dilated crypts and crypts with horizontal growth of the bases and no cytological dysplasia, consistent with the findings of SSA/P (Fig. 1b) [7, 8]. Figure 1c shows a representative endoscopic image of cancer in SSA/P with a slight central depression in the cecum. Histological examination revealed increased glandular density with crowded glands that had a back-to-back growth pattern and cells with rounded nuclei, coarse chromatin, and loss of polarity, consistent with the findings of cancer (Fig. 1d).

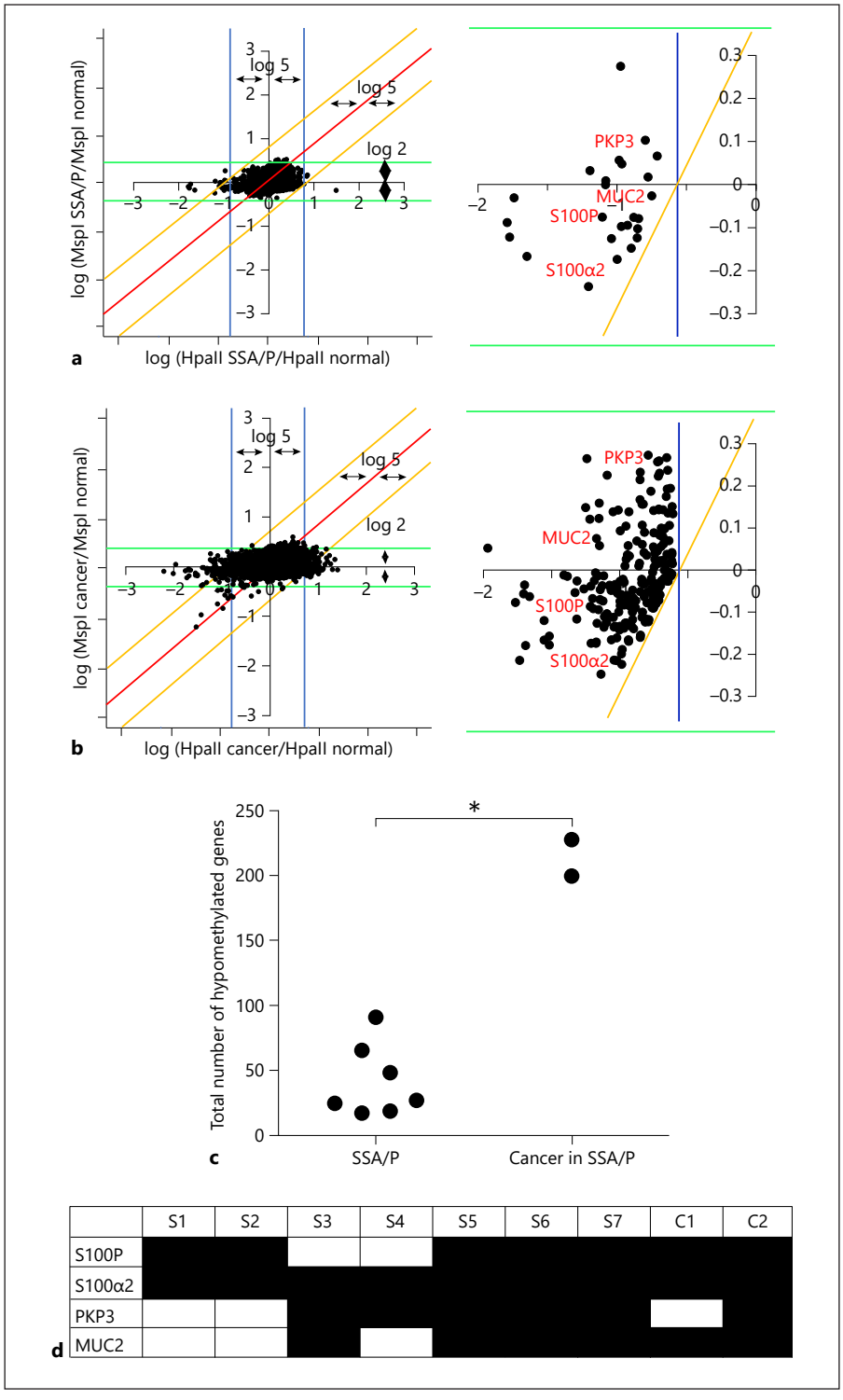

Fig. 2. Scatterplots of signals for each probe as determined using the microarray-based integrated analysis of methylation by isoschizomers (MIAMI) method, and the total number of hypomethylated genes and commonly hypomethylated genes in sessile serrated adenoma/polyp (SSA/P) and cancer in SSA/P tissues. **a**, **b** Green lines represent $y = \pm\log_2$, blue lines represent $x = \pm\log_5$, and yellow lines are located at $\pm\log_5$ horizontal distance from the regression line (red line) of the plots in accordance with the original MIAMI method of Hatada et al. [29]. Dots located within the 2 green lines and on the left side of the yellow line were determined to be hypomethylated in SSA/P (**a**) and cancer in SSA/P (**b**) tissues compared with paired normal colorectal epithelium. **c** The number of hypomethylated genes detected using the MIAMI method in 7 SSA/P and 2 cancer in SSA/P specimens was plotted. $*p < 0.05$. **d** The most commonly hypomethylated genes in 7 SSA/P specimens were S100P, S100α2, PKP3, and MUC2.

Hypomethylated Genes in SSA/P and Cancer in SSA/P Tissues

We investigated hypomethylated genes in SSA/Ps and cancer in SSA/P using genome-wide DNA methylation array analysis; 7 SSA/P and 2 cancers in SSA/P specimens were analyzed by the MIAMI method using the corresponding normal colonic epithelium as a reference. Representative scatter plots of the signals from

each probe in SSA/P (S1) and cancer in SSA/P specimens (C1) are shown in Figure 2a and b, respectively. The values for log ([Hpa II intensity] lesion/[Hpa II intensity] normal) are plotted on the *x*-axis, representing the relative methylation changes of each lesion. The values for the log ([Msp I intensity] lesion/[Msp l intensity] normal) are plotted on the *y*-axis, representing the control for the enzyme effects at sample digestion. The threshold values were determined according to the original MIAMI method described by Hatada et al. [29]. Dots located within the upper and lower green lines ($\pm\log_2$, respectively) and on the left side of the yellow line at $\log_5$ of the horizontal distance from the regression line of the plots represent hypomethylated genes in each lesion compared with paired normal colorectal epithelium: 27 genes were determined to be hypomethylated in the SSA/P specimens (Fig. 2a). Likewise, 228 genes were hypomethylated in cancer in SSA/P specimens (Fig. 2b). The mean number of hypomethylated genes in cancer in SSA/P specimens (214 ± 19.8) was significantly higher than that in SSA/P specimens (41.6 ± 27.5) (Fig. 2c, $p < 0.05$). Since we used normal colonic epithelium as a reference in the MIAMI analysis, our data indicated that the number of hypomethylated genes increases in a stepwise fashion from normal epithelia to SSA/P and then to cancer in SSA/P.

Of all the hypomethylated genes, S100α2, a calcium-binding protein, was hypomethylated in all SSA/P tissues (7/7, 100%) (Fig. 2d). S100P, a calcium-binding protein, and *PKP3*, a member of the armadillo multigene family, were hypomethylated in 5/7 (71.4%) samples. *MUC2*, a member of the mucin protein family, was hypomethylated in 4/7 (57.1%) samples. Moreover, all 4 genes were commonly hypomethylated in the 2 cancer in SSA/P samples except for PKP3 in 1 sample. The other genes were hypomethylated less frequently (≤3/7) or not hypomethylated. All SSA/P and cancer in SSA/P lesions were positive for BRAF mutation.

Levels of mRNA and Protein Expression of 4 Hypomethylated Genes

To validate the results of the hypomethylation array analysis, we first assessed the mRNA levels of the 4 genes in 10 additional SSA/P specimens using RT-PCR. The mRNA levels of S100P in SSA/P tissues were significantly higher than those in paired normal colon epithelium tissues ($p < 0.01$; Fig. 3a). Similarly, the levels of S100α2 and MUC2 in SSA/P tissues were significantly higher than those in paired normal colon epithelium tissues ($p < 0.05$; Fig. 3b, d). However, there was no significant difference in the mRNA levels of PKP3 between the SSA/P and normal colon epithelium tissues (Fig. 3c).

To determine whether protein expression of these 4 genes was upregulated by hypomethylation, we performed immunohistochemical staining using 5 SSA/P tissues with hypomethylation of each gene; representative staining patterns are shown in Figure 3e–h. S100P was intensely stained in the cytoplasm and nucleus of SSA/P cells but not in normal epithelial cells (Fig. 3e). S100α2 was weakly stained in the cytoplasm and nucleus of SSA/P cells, although it was also faintly stained in normal epithelial cells (Fig. 3f). PKP3 was stained mainly in the interstitial cells but very weakly in both SSA/P and normal epithelial cells (Fig. 3g). MUC2 was intensely stained in the cytoplasm of SSA/P cells but was also weakly stained in surrounding normal epithelial cells (Fig. 3h). Negative control was not stained in the cytoplasm of both SSA/P and normal epithelial cells (Fig. 3i). Although staining intensity for the 4 gene products was variable among the remaining 4 SSA/P specimens, it appeared that S100P was more intensely stained in most of the SSA/P samples than in surrounding normal epithelia (online suppl. Fig. 2). These results strongly suggest that hypomethylation of the S100P gene promotes its mRNA transcription and subsequent protein overexpression.

Inhibition of Cell Proliferation in Human SSA/P Organoids by Knockdown of S100P

To investigate the role of S100P in SSA/P cell proliferation, we established a human SSA/P organoids 1 and 2 from biopsy specimens, knocked down the S100P gene with lentiviral shRNA#1 and #2, and assessed cell proliferation using a cell viability assay. The level of S100P mRNA in SSA/P organoid cells transfected with a lentiviral shRNA#1 and #2 against S100P was decreased to only 10.0 ± 4.0% and 12.6 ± 2.3% of that in SSA/P organoid cells transfected with control shRNA, respectively (Fig. 4a, b). The viability of SSA/P organoid cells knocked down with S100P by lentiviral shRNA#1 and #2 was decreased to only 37.4 ± 2.7% and 34.1 ± 7.1% of that of control organoid cells at day 7 ($p < 0.01$; Fig. 4c, d). Moreover, we showed cell growth curves for the 2 strains of organoids introduced with S100P shRNA with the time course of cell proliferation in online suppl. Figure 3. The viability of SSA/P organoid cells with S100P knocked down was significantly lower compared with control cells treated with scramble shRNA at days 7 and 9. The mean diameter of SSA/P organoid 1 knocked down with S100P was significantly smaller (and) than that of control SSA/P organoid 1 (52.1 ± 24.9 vs. 139.6 ± 38.9 μm; $p < 0.01$; Fig. 4e, f).

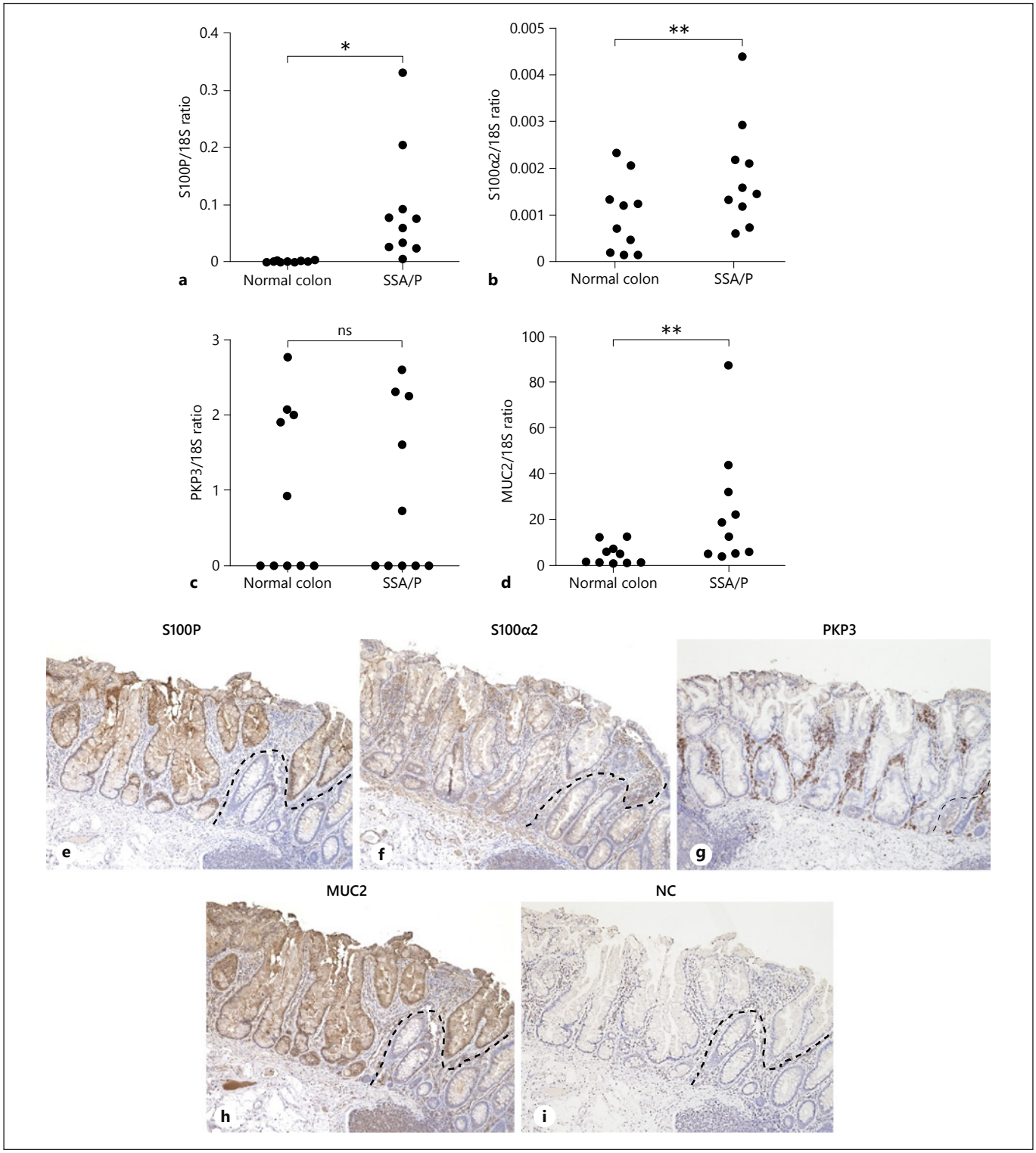

Fig. 3. Levels of mRNA and protein expression for S100P, S100α2, PKP3, and MUC2 in sessile serrated adenoma/polyp (SSA/P) tissues. **a–d** Relative mRNA levels of S100P (**a**), S100α2 (**b**), PKP3 (**c**), and MUC2 (**d**) in SSA/P and matched normal colorectal epithelium. The mRNA levels were determined by qRT-PCR and normalized to 18S RNA. *$p < 0.01$; **$p < 0.05$; ns, not significant. **e–i** Representative immunohistochemical staining for S100P (**e**), S100α2 (**f**), PKP3 (**g**), MUC2 (**h**), negative control (NC) (**i**). Magnification, ×100. The dotted line represents the border between SSA/P lesion and adjacent normal epithelia.

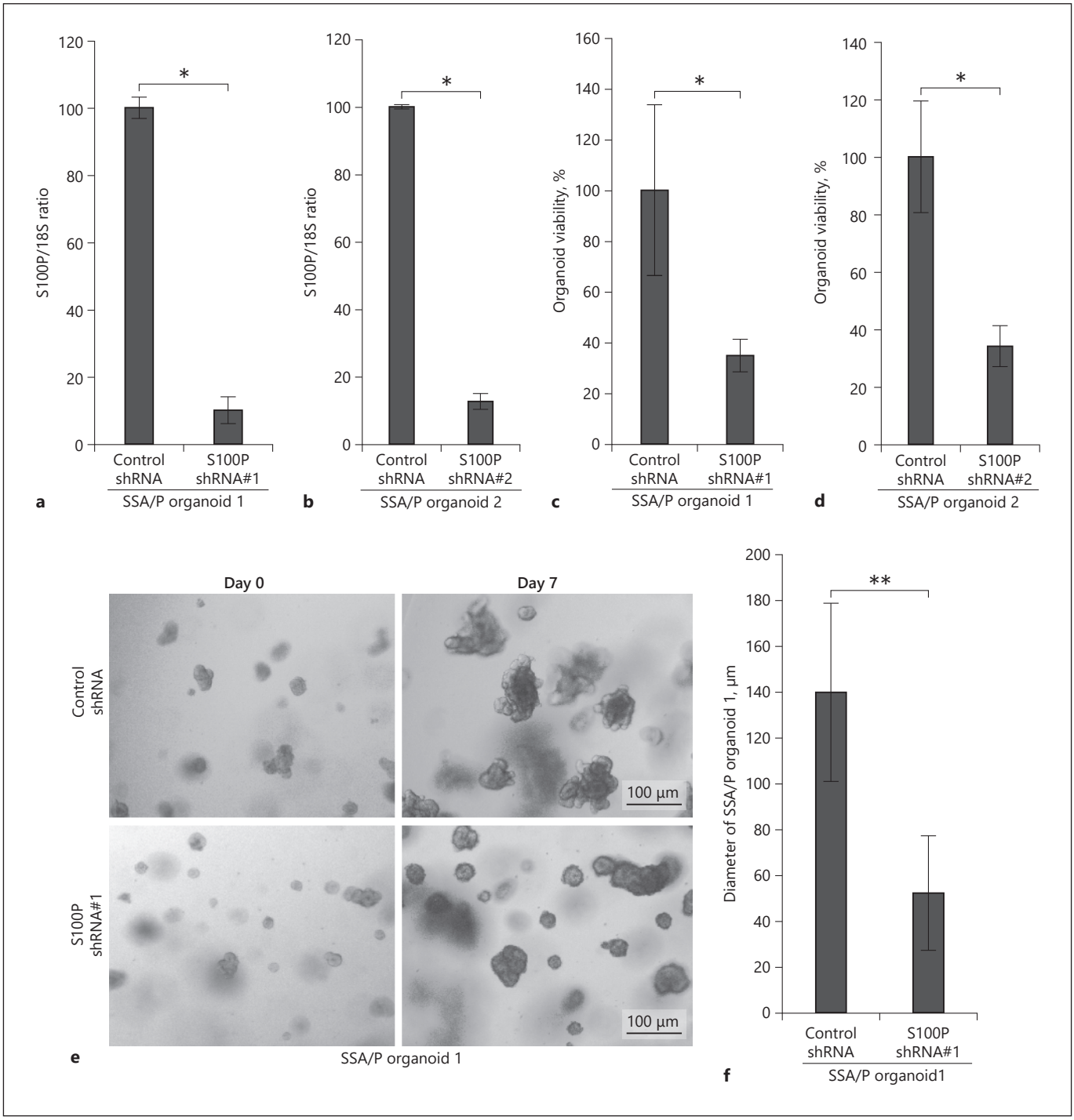

Fig. 4. Knockdown of S100P inhibited cell proliferation in sessile serrated adenoma/polyp (SSA/P) organoids. **a**, **b** SSA/P organoids 1 and 2 were transfected with S100P lentiviral shRNA#1 and #2 or control shRNA, and the knockdown efficiencies were assessed by qRT-PCR. **c**, **d** SSA/P organoid viability was assessed by CellTiter-Glo® assay at day 7. **e** Morphological findings of organoids with S100P shRNA#1 or control shRNA at day 0 and day 7. The organoids were chronologically observed and photographed using a microscope (magnification, ×400). **f** The average diameter of organoids was compared between organoids with S100P shRNA and control shRNA. *$p < 0.01$; **$p < 0.05$.

Similar results were obtained with SSA/P organoid 2 knocked down with S100P gene (44.3 ± 11.5 vs. 94.2 ± 23.4 μm; $p < 0.01$; online suppl. Fig. 3b, c). These data indicate that S100P promotes cell growth in SSA/P organoid cells.

We also examined the role of the S100P gene in the proliferation of CRC cell lines with BRAF mutation (HT29 and WiDr) by knocking down S100P with siRNA against S100P. The relative mRNA level of S100P in HT29 or WiDr cells transfected with siRNA was decreased to 17.8 ± 2.0% or 5.7 ± 0.4% of that in control cells at 72 h, respectively (Fig. 5a, e). Cell viability in HT29 and WiDr cells transfected with S100P siRNA was significantly decreased by 44.8 and 22.5% compared with control cells at 72 h, respectively ($p < 0.05$; Fig. 5c, g). Moreover, the mRNA level of S100P in HT29 or WiDr cells transfected with shRNA#1 was decreased to 4.6 ± 0.4% or 17.4 ± 1.0% of that in control cells at 72 h, respectively (Fig. 5a, e). The S100P protein expression in HT29 and WiDr cells transfected with S100P shRNA#1 was also obviously decreased, as revealed by Western blot analysis (online suppl. Fig. 5). Cell viability in HT29 or WiDr cells transfected with S100P shRNA#1 was significantly decreased by 18.5 and 26.9% compared with the control cells at 72 h, respectively ($p < 0.05$; Fig. 5d, h). These data indicate that S100P promotes cell growth not only in SSA/P but also in CRC cell lines.

Quantitative DNA Hypomethylation Analysis of S100P by MassARRAY

To quantitatively examine hypomethylation status in each of the 18 CpG sites in the S100P gene, we performed MassARRAY analysis on 3 SSA/P tissue samples using 3 probes for the 5′-flanking promoter region, exon 1, and intron 1 (Fig. 6a). A 2-way hierarchical clustering analysis showed differences in the methylation patterns of selected CpG sites in the S100P gene between SSA/P and corresponding normal tissue samples (Fig. 6b). Of the 18 CpG sites, 10 sites in SSA/P specimens exhibited significant hypomethylation rates as compared with corresponding normal epithelia ($p < 0.05$): 4 of 10 sites in the promoter region, 2 of 3 in exon 1, and 4 of 5 in intron 1. Detailed data on the methylation rates of each CpG site from the MassARRAY analysis are shown in online suppl. Table 4. The hypomethylation rates for the promoter region, exon 1, and intron 1 were 19.9 ± 15.3%, 16.1 ± 13.6%, and 28.3 ± 7.8%, respectively. Thus, hypomethylation of CpG sites occurred predominantly in intron 1 rather than in the promoter region or exon 1.

Discussion

In this study, we analyzed hypomethylated genes in SSA/P and cancer in SSA/P specimens using a genome-wide DNA methylation array and strongly suggested that DNA hypomethylation is closely associated with tumorigenesis in the SSA/P-cancer sequence. We have also successfully identified 4 commonly hypomethylated genes in SSA/Ps specimens; in particular, S100P showed significantly higher transcription and protein overexpression in SSA/P with hypomethylation at specific CpG sites as compared with surrounding normal epithelia. More importantly, we established 3-dimensional organoids from SSA/P specimens and showed that knockdown of the S100P gene significantly reduced the proliferation of SSA/P organoid cells in addition to the proliferation of BRAF-mutant CRC cell lines. These data clearly indicate that hypomethylation at specific CpG sites of the S100P gene plays an important role in the development of SSA/P.

It has been reported that DNA hypomethylation is generally associated with initiation of tumorigenesis, whereas DNA hypermethylation is associated with cancer progression [30, 31]. In this study, however, the mean number of hypomethylated genes in SSA/P and cancer in SSA/P specimens was 41.6 ± 27.5 and 214 ± 19.8, respectively. Since the normal colonic epithelium was used as a reference in this analysis, our data indicate that approximately 40 genes were hypomethylated during the formation of SSA/P and approximately 170 genes were hypomethylated during the formation of subsequent cancers. Thus, these data suggest that DNA hypomethylation would play a considerable role in the formation of cancer as well as the formation of precancerous SSA/P in the SSA/P-cancer sequence.

Renaud and colleagues [22] reported that intestinal mucin (MUC2) and gastric mucin (MUC5AC) genes were frequently hypomethylated in SSA/P but not in cancer tissues. We also found MUC2 hypomethylation in both SSA/P and cancer in SSA/P tissues but did not find MUC5AC hypomethylation in either tissue. It is unclear why our MUC5AC results differed from those of Renaud et al. [22]. Previous studies analyzed only a few genes for hypomethylation, whereas we performed genome-wide DNA methylation analysis and found 4 that were commonly hypomethylated (S100P, S100α2, PKP3, and MUC2). Importantly, our analysis included both SSA/P and "cancer in SSA/P tissues" to investigate epigenetic alterations in the SSA/P-cancer sequence.

S100P is a calcium-binding protein belonging to the S100 family and consisting of 95 amino acids [32]. It has been reported that S100P is expressed in several types of

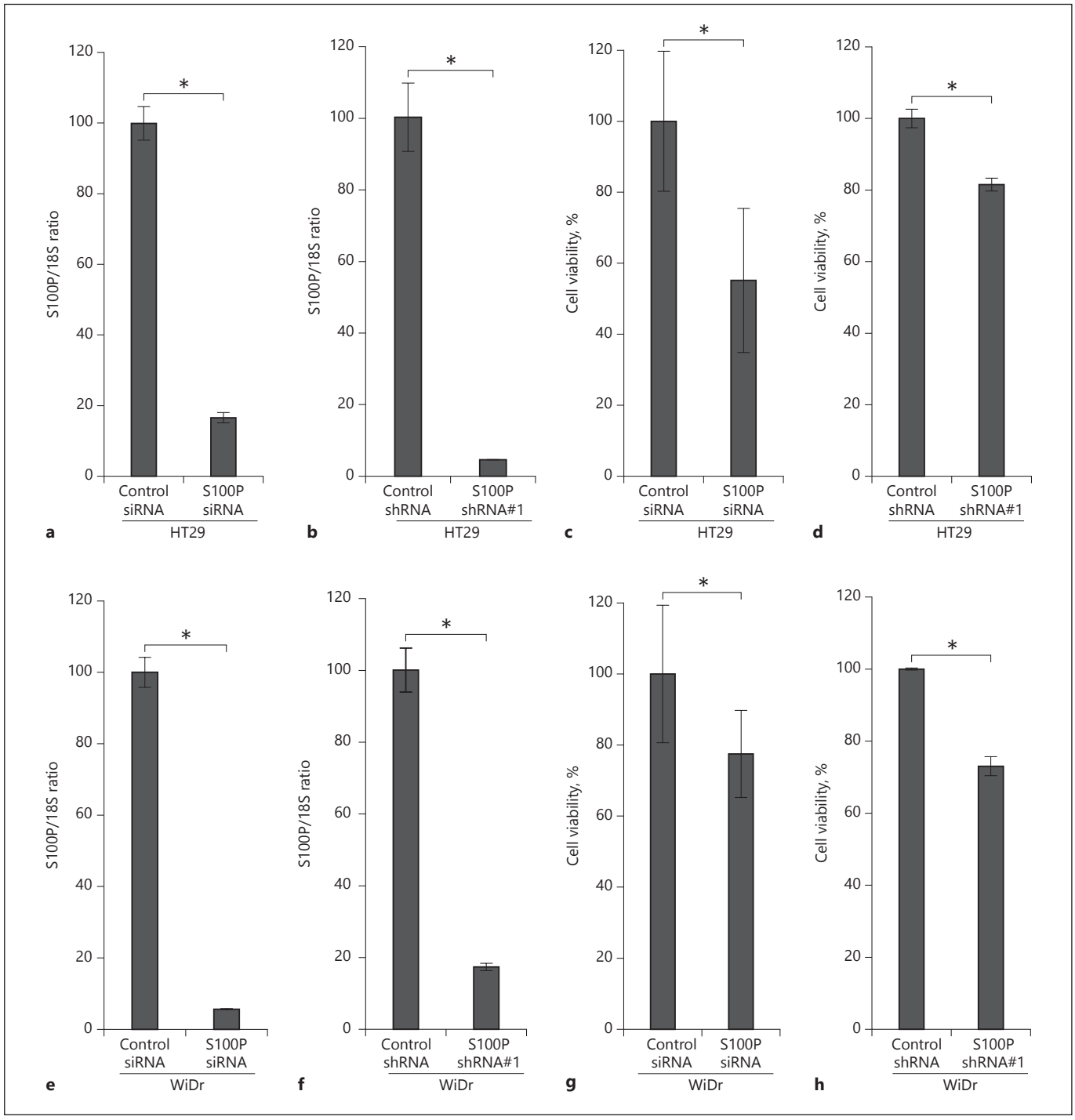

Fig. 5. Knockdown of S100P inhibited proliferation of BRAF-mutant colon cancer cell lines. **a**, **e** BRAF-mutant colon cancer cell lines HT29 (**a**) and WiDr (**e**) were transfected with small interfering RNA (siRNA) targeting S100P or scramble siRNA, and the knockdown efficiencies were assessed by qRT-PCR at 72 h after transfection. **c**, **g** Cell viability was assessed by BrdU assay in HT29 (**c**) and WiDr (**g**) at 72 h after transfection. *$p < 0.05$. **b**, **f** BRAF-mutant colon cancer cell lines HT29 (**b**) and WiDr (**f**) were transfected with S100P shRNA#1 or control shRNA, and the knockdown efficiencies were assessed by qRT-PCR PCR at 72 h after transfection. **d**, **h** Cell viability was assessed by BrdU assay in HT29 (**d**) and WiDr (**h**) at 72 h after transfection. *$p < 0.05$.

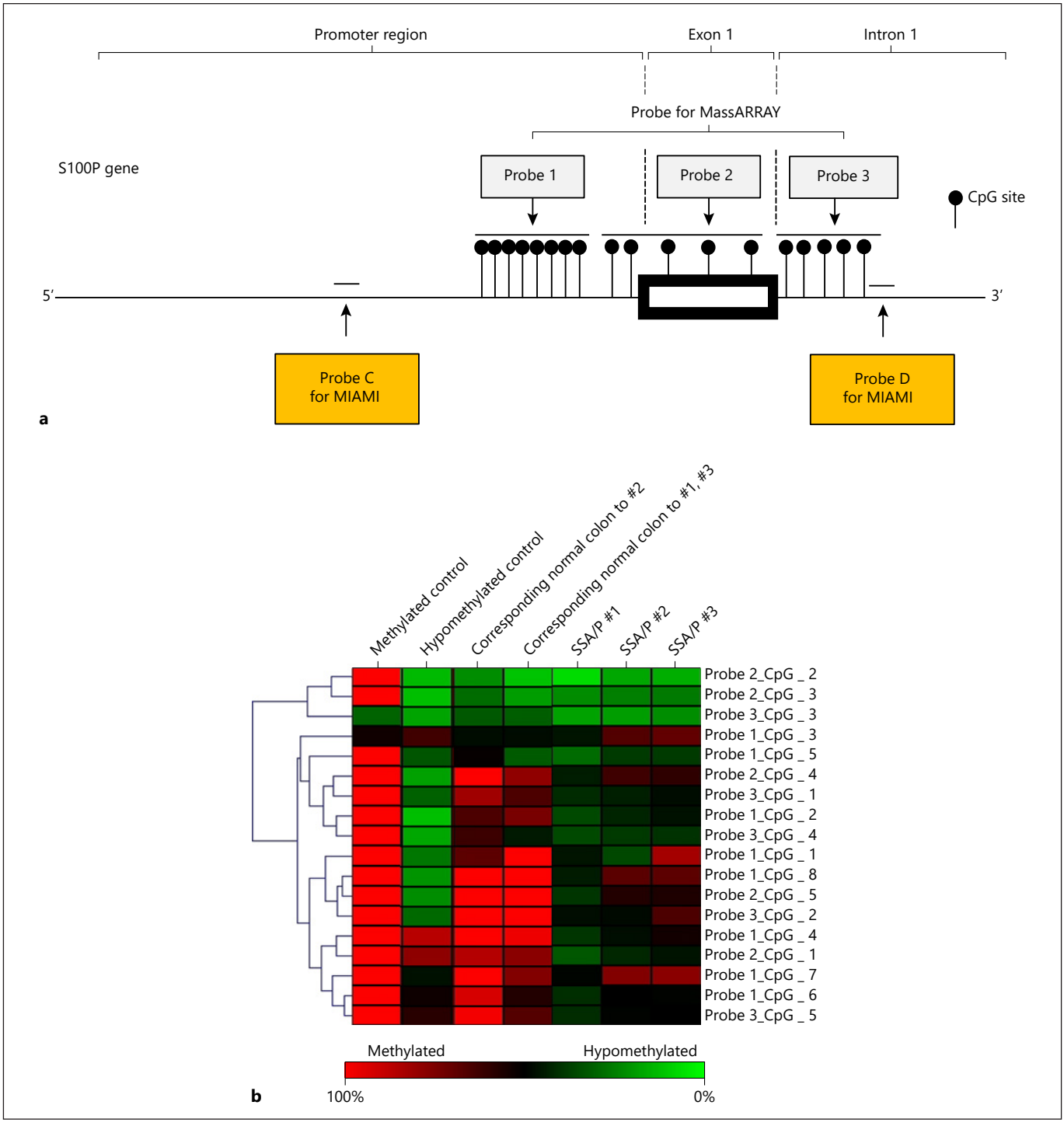

Fig. 6. CpG sites and probes for MassARRAY analysis in the S100P gene and cluster analysis of the relative hypomethylation of CpG units by MassARRAY analysis in sessile serrated adenoma/polyp (SSA/P) tissues. **a** Probes for MassARRAY analysis were set in the 5′-flanking promoter region, exon 1, and intron 1: probe 1 for 8 CpG sites in the promoter region, probe 2 for 2 CpG sites in the promoter regions and 3 CpG sites in the exon 1, and probe 3 for 5 CpG sites in the intron 1. Probes for MIAMI analysis were located in the promoter region (probe C) and in intron 1 (probe D). **b** Cluster analysis of the relative hypomethylation of 18 CpG units in the promoter, exon 1, and intron 1 of the S100P gene in SSA/P tissues compared with paired normal colonic epithelia by MassARRAY. Universally methylated DNA and unmethylated DNA from HCT116 cells were used as positive and negative controls, respectively (Torano et al. [20]).

cancers including those of the pancreas, breast, colon, prostate, and lung, and that S100P is associated with tumor growth, drug resistance, metastasis, and poor prognosis [30, 33–36]. Jiang and colleagues [37] reported that knockdown of the S100P gene in CRC cell lines (DLD1 and SW620) inhibited proliferation, migration, and invasion in vitro and in a xenograft model. The inhibition of proliferation by knockdown of S100P in CRC cell lines is consistent with our results. However, no study has been able to show the functional role of S100P gene in precancerous lesions such as SSA/P and/or adenoma, because there was no suitable culture model of benign tumors available, unlike with CRCs. We established 3-dimensional organoids from SSA/P specimens, as we reported recently [38], and showed that knockdown of the S100P gene using lentivirus-mediated shRNA significantly inhibited the proliferation of SSA/P organoids. S100P knockdown inhibited cell growth by approximately 63% in SSA/P organoids, whereas it inhibited cell growth by only 23–45% in BRAF-mutant CRC cell lines. Although these values are not simply comparable, our results suggest that S100P may play a more important role in the growth of SSA/P than cancer cells. In addition, Fuentes and colleagues [39] reported that addition of exogenous S100P stimulates proliferation and migration of SW480 CRC cells by its binding to cell surface RAGE (S100P/RAGE signaling pathway), which subsequently activates MAP kinase and NF-kB pathways. We also confirmed the RAGE expression in SSA/P organoids and CRC cells with BRAF mutation (HT29/WiDr), as well as in SSAP tissues and cancer in SSA/P specimens using Western blot analysis and immunohistochemistry (online suppl. Fig. 4). These results may explain the developmental mechanism of SSA/P through accumulated DNA hypomethylation and hypermethylation with BRAF mutation. In particular, expression of S100P due to hypomethylation would confer a significant cell growth advantage via the S100P/RAGE signaling pathway during the formation of SSA/P. Moreover, we found that expressions of p-Erk (a member of MAP kinase) in WiDr and HT29 cells were slightly inhibited by S100P shRNA-introduction but expressions of pp65, a subunit of NF-KB, were unchanged (online suppl. Fig. 5). Therefore, it is possible that RAGE pathway may be activated by MAP kinase pathway.

Sato and colleagues [28] reported that hypomethylation of S100P and maspin is a common epigenetic alteration in pancreatic cancer. They also found specific hypomethylation of CpG sites in the 5′-flanking promoter region and part of exon 1 of the S100P gene. However, the area and degree of hypomethylation at CpG sites in the S100P gene were undetermined. In the present study, quantitative MassARRAY analysis showed that hypomethylated CpG sites were predominantly located in intron 1 rather than in the promoter and in exon 1 of the S100P gene. These results indicate that hypomethylation at the CpG sites in intron 1 as well as in exon 1 and the promoter region of the S100P gene probably induce elevated transcription and subsequent overexpression of S100P protein, resulting in enhanced cell growth during the formation of SSA/P.

Expression of MUC2 and S100α2 mRNAs, in addition to S100P mRNA, was significantly elevated in SSA/P tissues, probably due to hypomethylation. Since MUC2 expression has been implicated in the progression of microvesicular hyperplastic polyp to SSA/P [22], it is plausible that MUC2 expression may play an important role in the serrated-neoplasia pathway. However, the precise role and significance of these genes should be elucidated in future studies. As a limitation of this study, the number of samples, particularly the number of cancer in SSA/P tissues examined, were small. Therefore, it will be important to confirm the data using more samples in future.

Conclusion

Our results suggest that global DNA hypomethylation, including S100P hypomethylation, is supposedly associated with the SSA/P-cancer sequence. S100P, which is overexpressed due to hypomethylation at specific CpG sites in intron 1, exon 1, and the 5′-promoter region, plays an important role in cell proliferation in SSA/P. S100P may therefore be a novel therapeutic and prophylactic target for SSA/P and subsequent cancer.

Acknowledgements

We thank Prof. Takanori Kanai (Department of Gastroenterology, Keio University School of Medicine) for assistance with organoid culture. We are also grateful to Drs. J. Shunto (Tokushima, Japan) and K. Kataoka (Tokushima, Japan) for referring SSA/P patients to our hospital, and Y. Okamoto, H. Nakanishi, and S. Takeishi for their expert technical assistance for experiments.

Statement of Ethics

This study was approved by the Ethics Committee of Tokushima University Hospital (approval number 895). Written informed consent was obtained prior to colonoscopy from all patients who had been known or suspected to have SSA/P.

Conflict of Interest Statement

The authors disclose no conflicts.

Funding Sources

This work was partly supported by a Grant-in-Aid for Scientific Research from the Japan Society for the Promotion of Science (JSPS; grant number 24590942).

Author Contributions

S.T. and T. Takayama designed the research. S.T., K.O., S.F., T.N., T.K., Y.F., Y.M., S.K, and H.M. performed experiments. T. Tanahashi, Y.S., and N.M. analyzed the data and drafted the manuscript. Y.B. and T.F. performed pathological diagnosis. T.S. assisted with the establishment of 3-dimensional organoid. S.T., K.O., M.B., and B.M. performed in vitro experiments with organoid cells. All authors contributed to the writing and approved the final manuscript.

References

1 Bray F, Ferlay J, Soerjomataram I, Siegel RL, Torre LA, Jemal A. Global cancer statistics, 2018: GLOBOCAN estimates of incidence and mortality worldwide for 36 cancers in 185 countries. CA Cancer J Clin. 2018;68:394–424.
2 Vogelstein B, Fearon ER, Hamilton SR, Kern SE, Preisinger AC, Leppert M, et al. Genetic alterations during colorectal-tumor development. N Engl J Med. 1988;319(9):525–32.
3 Snover DC. Update on the serrated pathway to colorectal carcinoma. Hum Pathol. 2011;42(1):1–10.
4 Jass JR. Classification of colorectal cancer based on correlation of clinical, morphological and molecular features. Histopathology. 2007;50(1):113–30.
5 Sugai T, Habano W, Takagi R, Yamano H, Eizuka M, Arakawa N, et al. Analysis of molecular alterations in laterally spreading tumors of the colorectum. J Gastroenterol. 2017;52(6):715–23.
6 Cancer Genome Atlas Network. Comprehensive molecular characterization of human colon and rectal cancer. Nature. 2012;487(7407):330–7.
7 Snover DC, Ahnen DJ, Burt RW, Odze RD. Serrated polyps of the colon and rectum and serrated polyposis. In: WHO classification of tumours of the digestive system. 4th ed. Lyon, France: IARC; 2010. p. 160–5.
8 Pai RK, Makinen MJ, Rosty C. Colorectal serrated lesions and polyps. In: WHO classification of tumours of the digestive system. 5th ed. Lyon, France: IARC; 2019. p. 163–9.
9 Kambara T, Simms LA, Whitehall VL, Spring KJ, Wynter CV, Walsh MD, et al. BRAF mutation is associated with DNA methylation in serrated polyps and cancers of the colorectum. Gut. 2004;53(8):1137–44.
10 Higuchi T, Sugihara K, Jass JR. Demographic and pathological characteristics of serrated polyps of colorectum. Histopathology. 2005;47(1):32–40.
11 O'Brien MJ, Yang S, Mack C, Xu H, Huang CS, Mulcahy E, et al. Comparison of microsatellite instability, CpG island methylation phenotype, BRAF and KRAS status in serrated polyps and traditional adenomas indicates separate pathways to distinct colorectal carcinoma end points. Am J Surg Pathol. 2006;30:1491–501.
12 Rosty C, Hewett DG, Brown IS, Leggett BA, Whitehall VL. Serrated polyps of the large intestine: current understanding of diagnosis, pathogenesis, and clinical management. J Gastroenterol. 2013;48(3):287–302.
13 Bettington M, Walker N, Clouston A, Brown I, Leggett B, Whitehall V. The serrated pathway to colorectal carcinoma: current concepts and challenges. Histopathology. 2013;62(3):367–86.
14 Toyota M, Ahuja N, Ohe-Toyota M, Herman JG, Baylin SB, Issa JP. CpG island methylator phenotype in colorectal cancer. Proc Natl Acad Sci U S A. 1999;96(15):8681–6.
15 Cunningham JM, Christensen ER, Tester DJ, Kim CY, Roche PC, Burgart LJ, et al. Hypermethylation of the hMLH1 promoter in colon cancer with microsatellite instability. Cancer Res. 1998;58(15):3455–60.
16 Kriegl L, Neumann J, Vieth M, Greten FR, Reu S, Jung A, et al. Up and downregulation of p16(Ink4a) expression in BRAF-mutated polyps/adenomas indicates a senescence barrier in the serrated route to colon cancer. Mod Pathol. 2011;24(7):1015–22.
17 Inoue A, Okamoto K, Fujino Y, Nakagawa T, Muguruma N, Sannomiya K, et al. B-RAF mutation and accumulated gene methylation in aberrant crypt foci (ACF), sessile serrated adenoma/polyp (SSA/P) and cancer in SSA/P. Br J Cancer. 2015;112(2):403–12.
18 Liu C, Fennell LJ, Bettington ML, Walker NI, Dwine J, Leggett BA, et al. DNA methylation changes that precede onset of dysplasia in advanced sessile serrated adenomas. Clin Epigenetics. 2019;11(1):90.
19 Matsuzaki K, Deng G, Tanaka H, Kakar S, Miura S, Kim YS. The relationship between global methylation level, loss of heterozygosity, and microsatellite instability in sporadic colorectal cancer. Clin Cancer Res. 2005;11(24 Pt 1):8564–9.
20 Torano EG, Petrus S, Fernandez AF, Fraga MF. Global DNA hypomethylation in cancer: review of validated methods and clinical significance. Clin Chem Lab Med. 2012;50:1733–42.
21 Cui H, Onyango P, Brandenburg S, Wu Y, Hsieh CL, Feinberg AP. Loss of imprinting in colorectal cancer linked to hypomethylation of H19 and IGF2. Cancer Res. 2002;62(22):6442–6.
22 Renaud F, Mariette C, Vincent A, Wacrenier A, Maunoury V, Leclerc J, et al. The serrated neoplasia pathway of colorectal tumors: identification of MUC5AC hypomethylation as an early marker of polyps with malignant potential. Int J Cancer. 2016;138(6):1472–81.
23 Sato T, Stange DE, Ferrante M, Vries RG, Van Es JH, Van den Brink S, et al. Long-term expansion of epithelial organoids from human colon, adenoma, adenocarcinoma, and Barrett's epithelium. Gastroenterology. 2011;141(5):1762–72.
24 Maru Y, Orihashi K, Hippo Y. Lentivirus-based stable gene delivery into intestinal organoids. Methods Mol Biol. 2016;1422:13–21.
25 Zhang Z, Wang H, Ding Q, Xing Y, Xu Z, Lu C, et al. Establishment of patient-derived tumor spheroids for non-small cell lung cancer. PLoS One. 2018;13(3):e0194016.
26 Tomonari T, Takeishi S, Taniguchi T, Tanaka T, Tanaka H, Fujimoto S, et al. MRP3 as a novel resistance factor for sorafenib in hepatocellular carcinoma. Oncotarget. 2016;7(6):7207–15.
27 Fuchikami M, Morinobu S, Segawa M, Okamoto Y, Yamawaki S, Ozaki N, et al. DNA methylation profiles of the brain-derived neurotrophic factor (BDNF) gene as a potent diagnostic biomarker in major depression. PLoS One. 2011;6(8):e23881.
28 Sato N, Fukushima N, Matsubayashi H, Goggins M. Identification of maspin and S100P as novel hypomethylation targets in pancreatic cancer using global gene expression profiling. Oncogene. 2004;23(8):1531–8.
29 Hatada I, Fukasawa M, Kimura M, Morita S, Yamada K, Yoshikawa T, et al. Genome-wide profiling of promoter methylation in human. Oncogene. 2006;25(21):3059–64.

30 Hernandez-Blazquez FJ, Habib M, Dumollard JM, Barthelemy C, Benchaib M, de Capoa A, et al. Evaluation of global DNA hypomethylation in human colon cancer tissues by immunohistochemistry and image analysis. Gut. 2000;47(5):689–93.
31 Frigola J, Solé X, Paz MF, Moreno V, Esteller M, Capellà G, et al. Differential DNA hypermethylation and hypomethylation signatures in colorectal cancer. Hum Mol Genet. 2005; 14(2):319–26.
32 Becker T, Gerke V, Kube E, Weber K. S100P, a novel Ca2+-binding protein from human placenta. cDNA cloning, recombinant protein expression and Ca2+ binding properties. Eur J Biochem. 1992;207(2):541–7.
33 Arumugam T, Logsdon CD. S100P: a novel therapeutic target for cancer. Amino Acids. 2011;41(4):893–9.
34 Diederichs S, Bulk E, Steffen B, Ji P, Tickenbrock L, Lang K, et al. S100 family members and trypsinogens are predictors of distant metastasis and survival in early-stage non-small cell lung cancer. Cancer Res. 2004; 64(16):5564–9.
35 Surowiak P, Maciejczyk A, Materna V, Drag-Zalesińska M, Wojnar A, Pudelko M, et al. Unfavourable prognostic significance of S100P expression in ovarian cancers. Histopathology. 2007;51(1):125–8.
36 Mousses S, Bubendorf L, Wagner U, Hostetter G, Kononen J, Cornelison R, et al. Clinical validation of candidate genes associated with prostate cancer progression in the CWR22 model system using tissue microarrays. Cancer Res. 2002;62(5):1256–60.
37 Jiang L, Lai YK, Zhang J, Wang H, Lin MC, He ML, et al. Targeting S100P inhibits colon cancer growth and metastasis by Lentivirus-mediated RNA interference and proteomic analysis. Mol Med. 2011;17(7–8):709–16.
38 Fujii M, Shimokawa M, Date S, Takano A, Matano M, Nanki K, et al. A colorectal tumor organoid library demonstrates progressive loss of niche factor requirements during tumorigenesis. Cell Stem Cell. 2016;18(6):827–38.
39 Fuentes MK, Nigavekar SS, Arumugam T, Logsdon CD, Schmidt AM, Park JC, et al. RAGE activation by S100P in colon cancer stimulates growth, migration, and cell signaling pathways. Dis Colon Rectum. 2007;50(8): 1230–40.